SUPPLEMENTARY INFORMATION

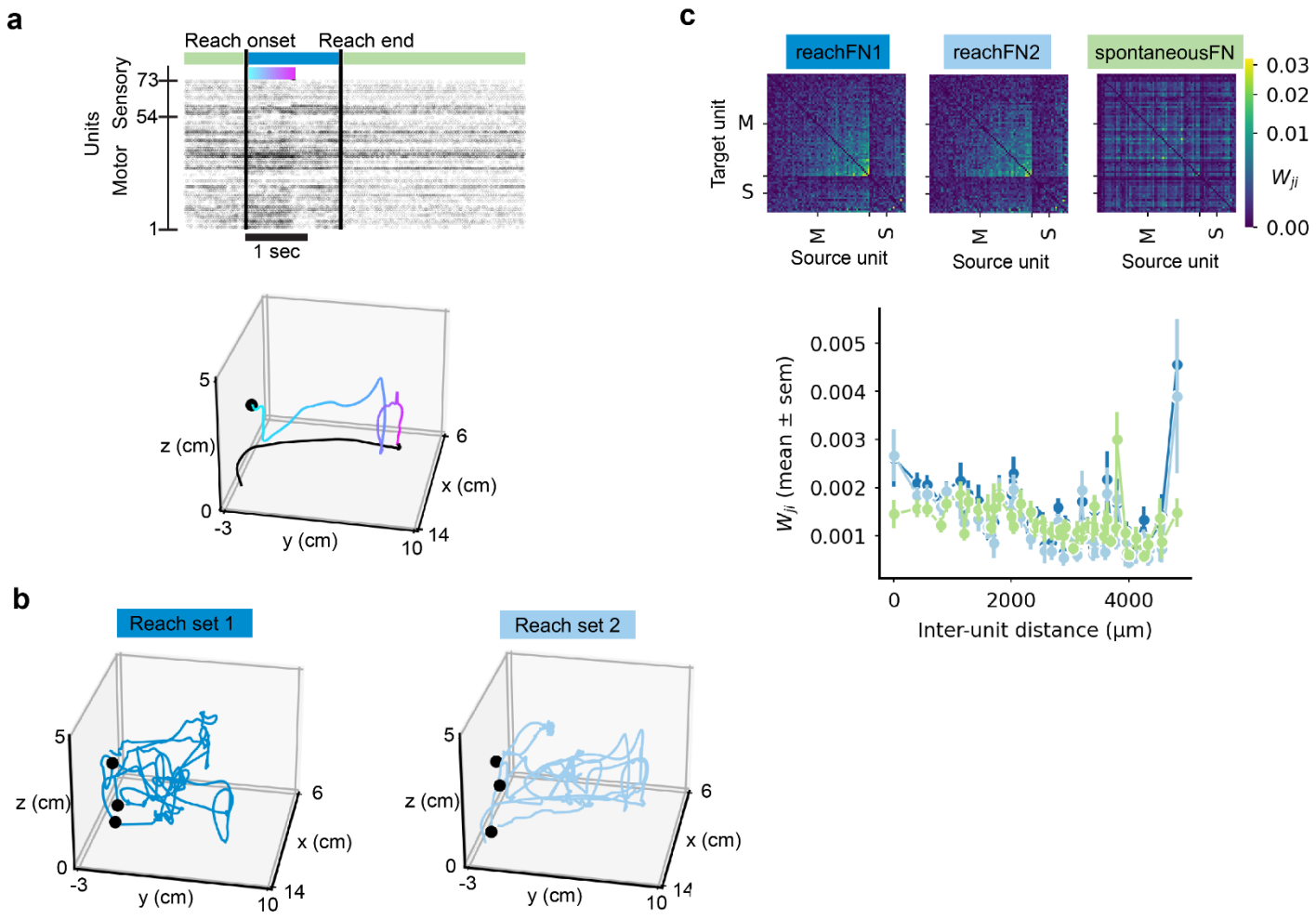

Supplementary Figure 1. MG data. (A-C) Data presentation and legends identical to Fig. 1. (A) Top: Raster plot from reach 14 of MG recording. Bottom: wrist position (black) from reach onset (black dot) to reach end, with the color gradient indicating neural modulation in the top panel imposed on the kinematics. (B) Sample of 6 of 56 reaches. (C) Top: FNs computed for MG. Bottom: Edge weights (mean ± sem) versus inter-electrode distance in the computed FNs, with sample numbers ranging from 2 samples at 4,816 μm to 159 samples at 400 μm (individual sample numbers are available in the Source Data file).

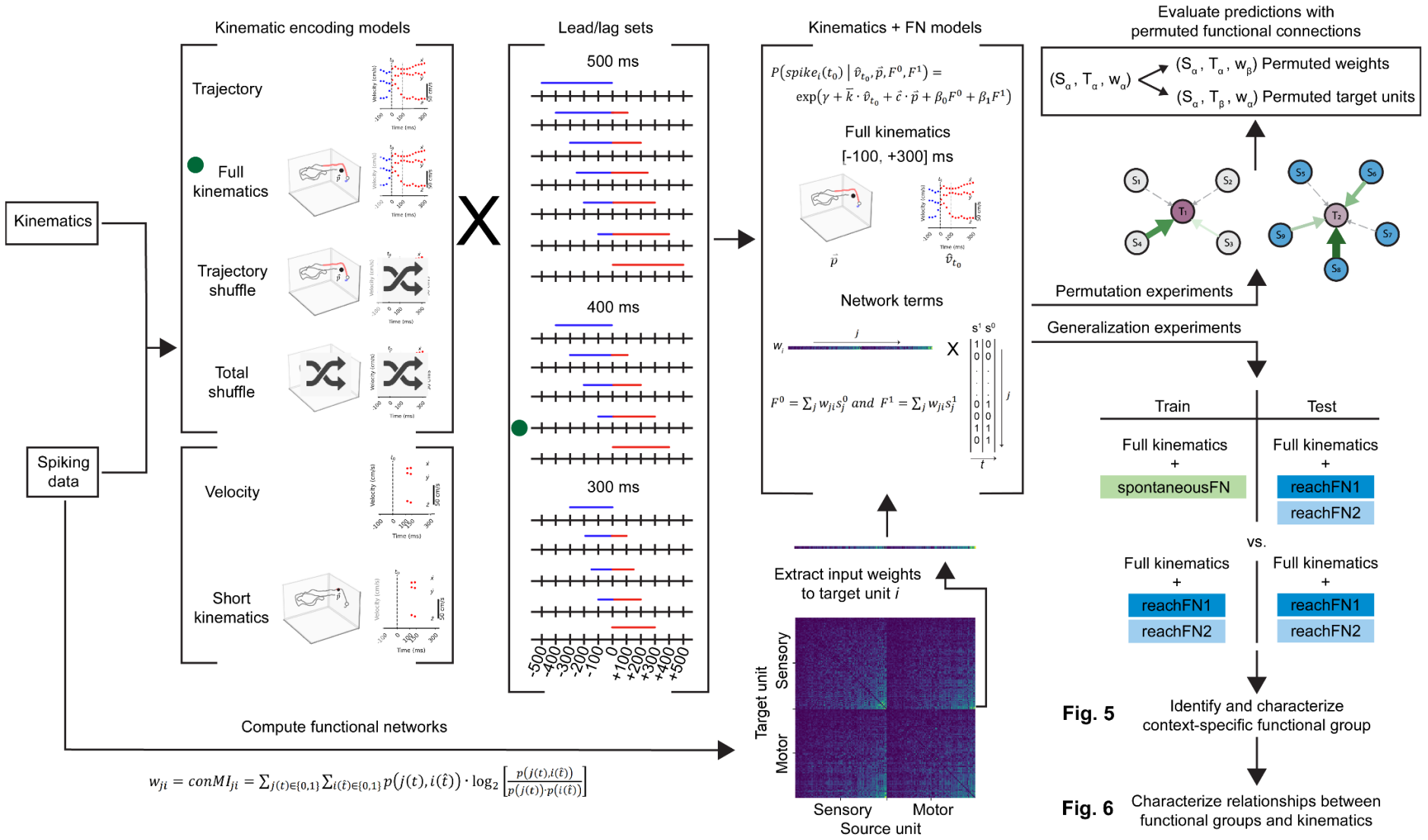

Supplementary Figure 2. Analysis flow chart. Analysis begins at the left with hand kinematics and spiking data, as shown in Fig. 1. Next, kinematic encoding models were tested over 17 lead/lag sets (results shown in Fig. 2). We selected the Full Kinematics model with trajectories sampled in [-100, +300]ms for further analysis (selections are marked by green circles). Next, the FN was computed from spiking data using the confluent mutual information between pairs of units (bottom left). Network terms were incorporated into the model for a target unit i by multiplying the row of weights from all source units j to target unit i with the columns of spike activity in source unit j for the preceding and current time bin (s^1 and s^0, respectively). Results related to this model are shown in Fig. 3. Next, we conducted permutation experiments in which the top N% of strongest connections were manipulated by permuting either the weights or target units within the group. These results, shown in Fig. 4, were compared to manipulation of random connections and to removal of all network terms to assess whether prediction of spikes depended on the topology of strong connections. Finally, we conducted generalization experiments in which we compared performance of models trained with network terms computed from the spontaneousFN to models correctly trained on the reachFN1/2. These experiments revealed a context-specific functional group. We describe and characterize the functional group and its relationship to kinematic tuning in Fig. 5 and Fig. 6.

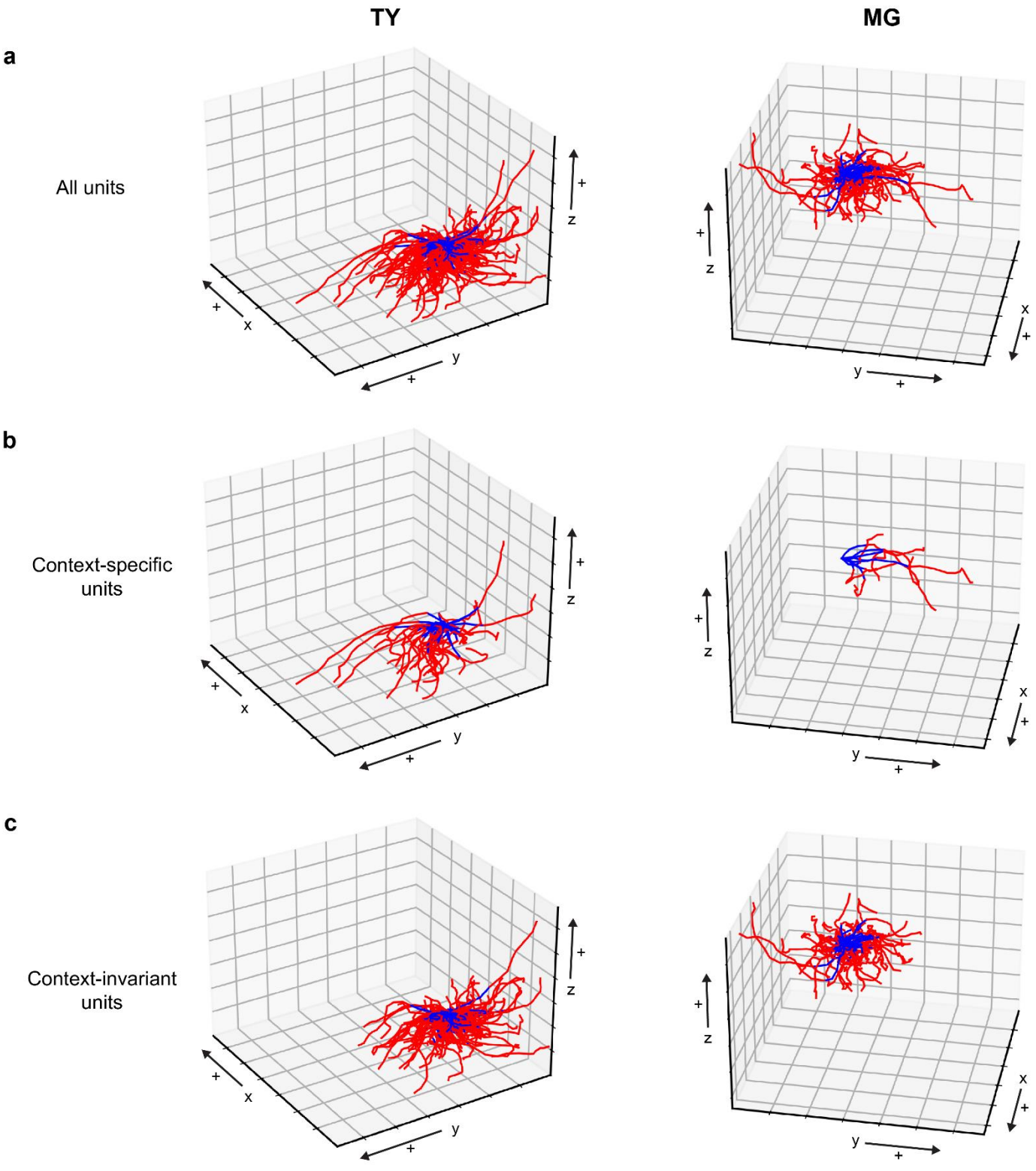

Supplementary Figure 3. Preferred trajectory pathlets. (A-C) Left: TY, Right: MG. (A) The average pathlet for each unit with -100ms of lead kinematics in blue and +300ms of lag kinematics in red. The positive y-axis moves into the prey-capture box. (B) Pathlets of units in the context-specific functional group. (C) Pathlets of units in the context-invariant functional group.

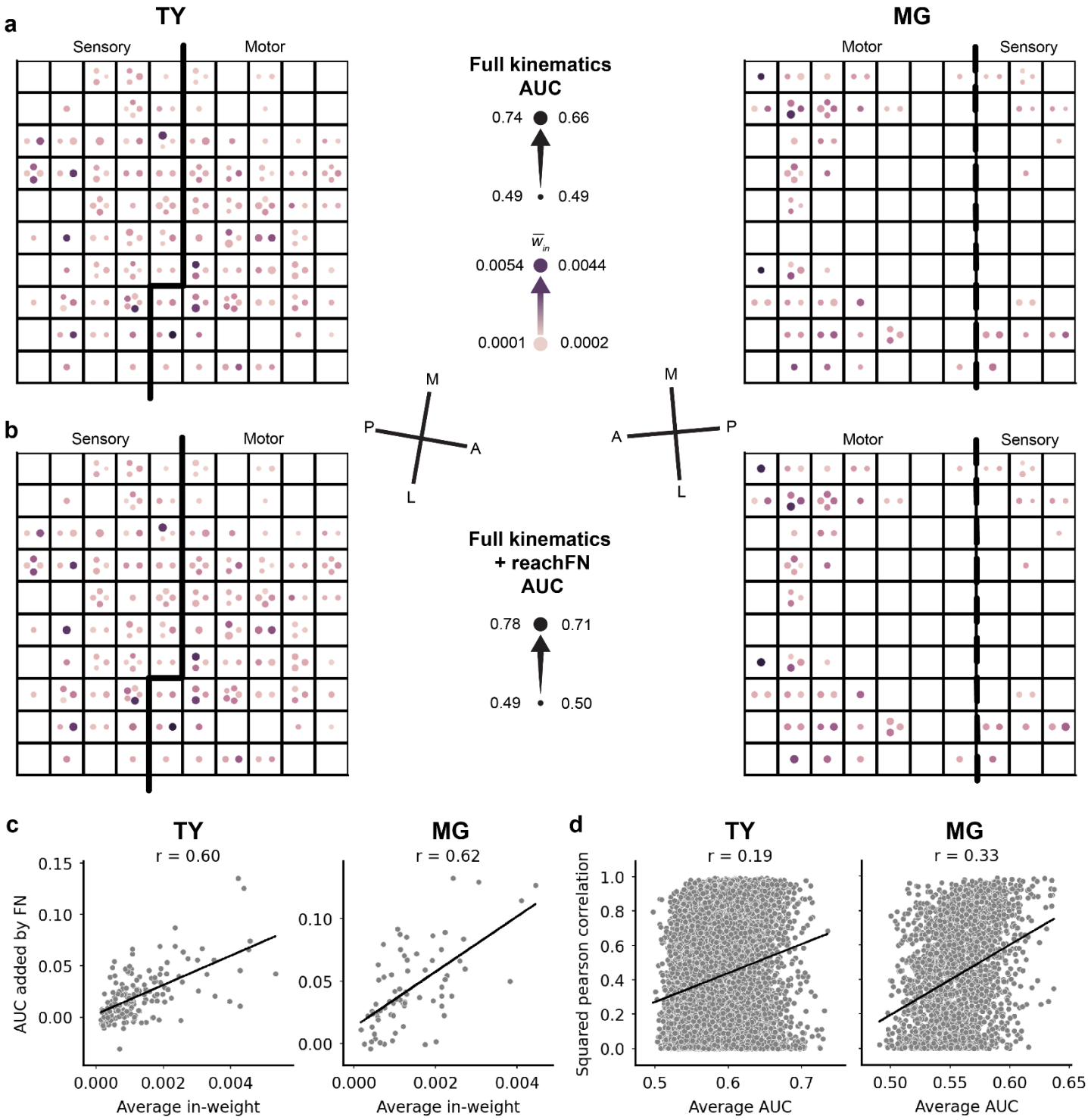

Supplementary Figure 4. Additional model results. (A) Results of the full kinematics model on the array. Dot size and dot hue indicate the AUC and average in-weight, respectively, for each unit. The dashed-line boundary between motor and sensory areas for monkey MG indicates less confidence in the precise location of the boundary compared to monkey TY (see Methods). The cardinal axes in cortex were estimated from surgical photos and are denoted medial (M), lateral (L), anterior (A) and posterior (P). (B) The kinematics+reachFN model results on the array. (C) Scatterplots showing a strong positive correlation between improvement in AUC from the full kinematics model to the kinematics+reachFN model and average in-weight to the unit for TY (left) and MG (right). (D) Scatterplots of pairwise preferred trajectory correlation squared versus average AUC of the unit pair, showing a weak positive correlation.

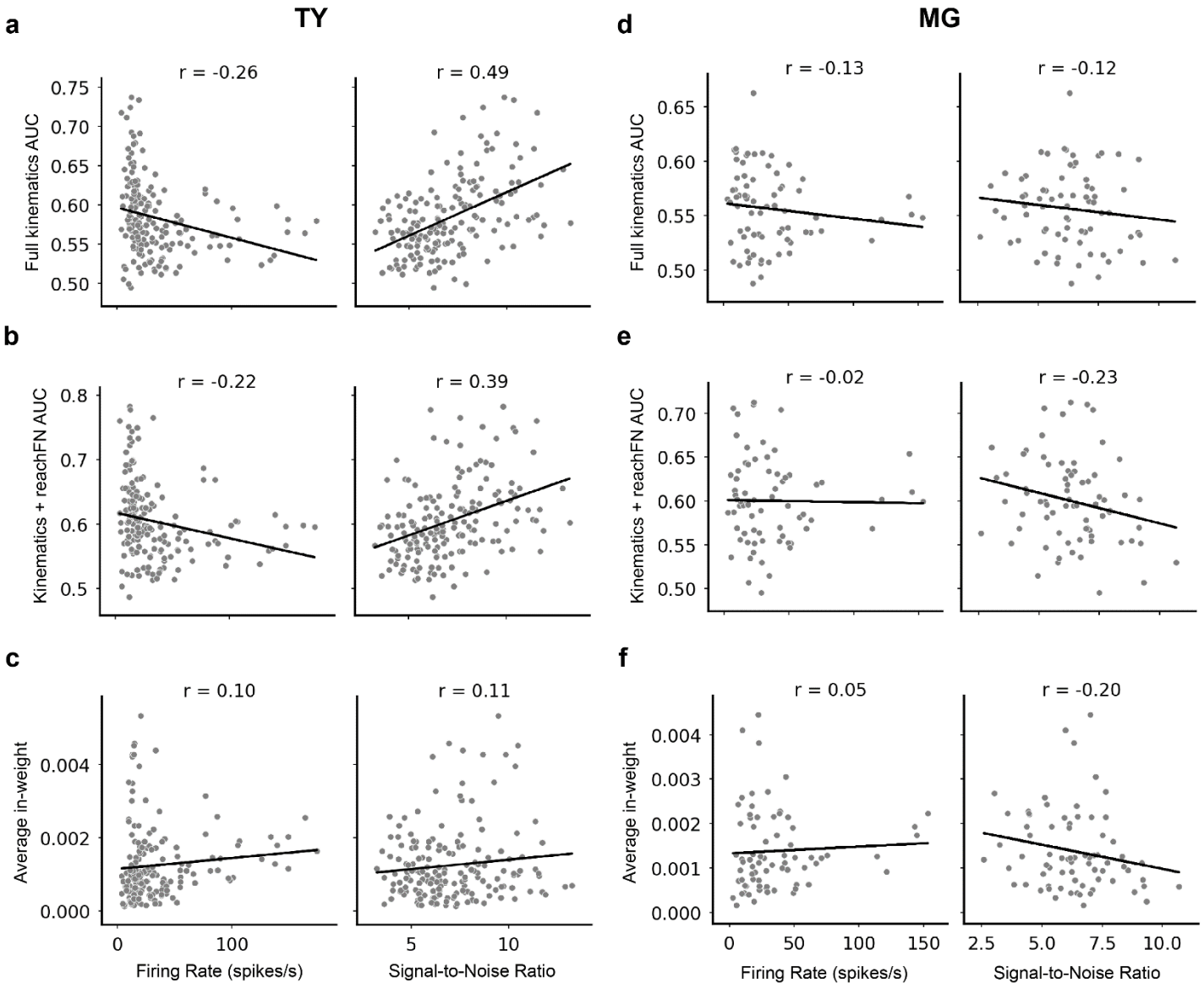

Supplementary Figure 5. Checks of potential confounds. (A-C) Monkey TY. (A) Scatterplots showing weak negative correlation between AUC of the full kinematics model and firing rate (left) and a positive correlation with signal-to-noise ratio (SNR; right). (B) Similar correlation of kinematics+reachFN AUC with firing rate and SNR. (C) Negligible correlation of average in-weight with firing rate and SNR. (D-F) Monkey MG. (D) Negligible correlation of full kinematics AUC and both firing rate and SNR. (E) No correlation between kinematics+reachFN AUC and firing rate. Weak negative correlation with SNR, which is opposite from TY result. (F) No correlation of average in-weight with firing rate. Weak negative correlation with SNR.

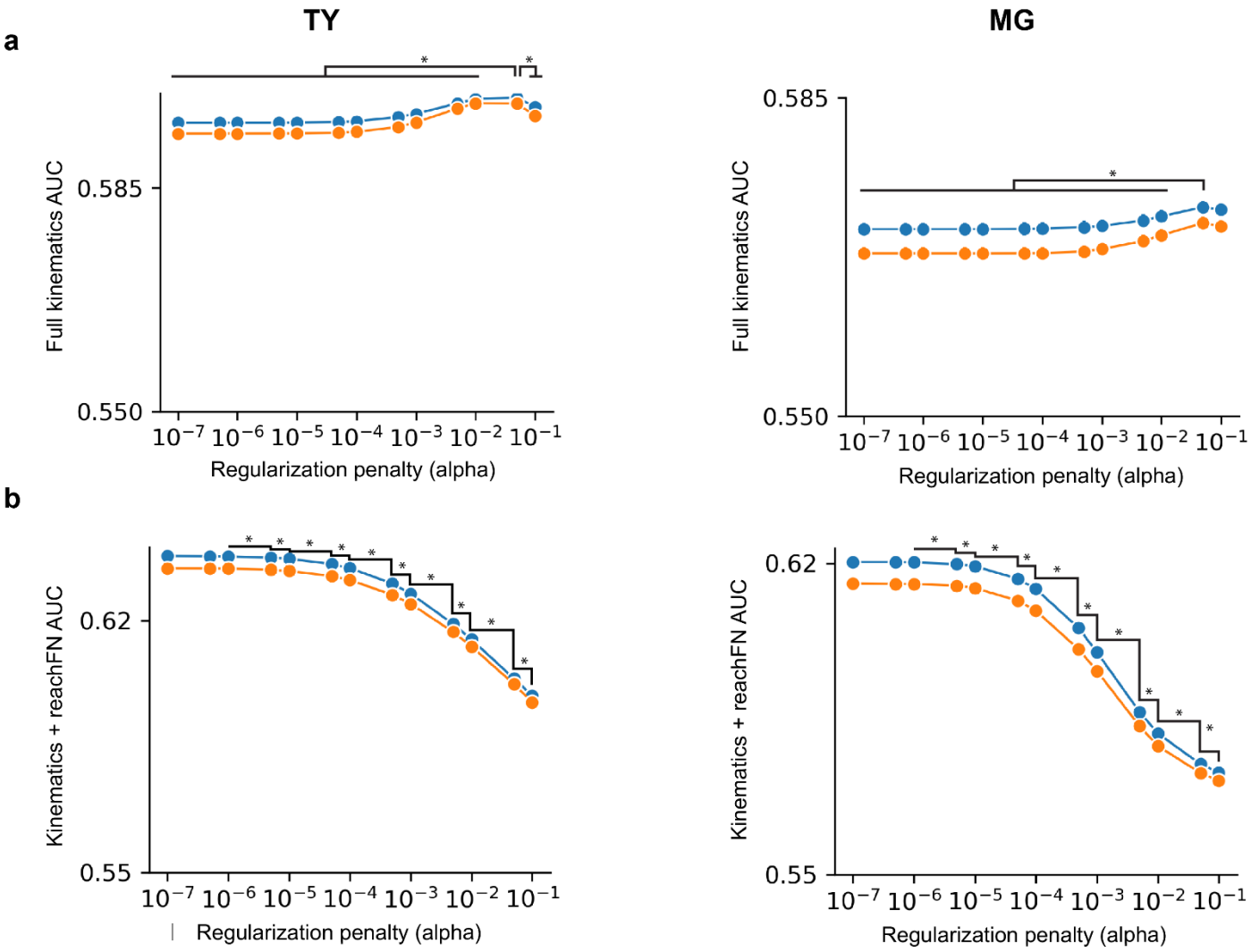

Supplementary Figure 6. L2-regularization penalty weight sweep. (A-B) Left: monkey TY, right: monkey MG. (A) AUC (mean ± sem) for full kinematics model on held-out test data for all units and train/test splits for lead/lag sets [-100, +300]ms (blue) and [-200, +300]ms (orange). Values of α that produced significantly lower AUC values than $\alpha = 0.05$ are indicated by the * ($p<0.05$, one-sided sign test). (B) Same for the kinematics+reachFN model. Steps marked with * indicate a decrease in α that produced significantly higher AUC values ($p < 0.05$, one-sided sign test). For both monkeys, changes to α no longer provided performance improvements for $\alpha < 1 \times 10^{-6}$.

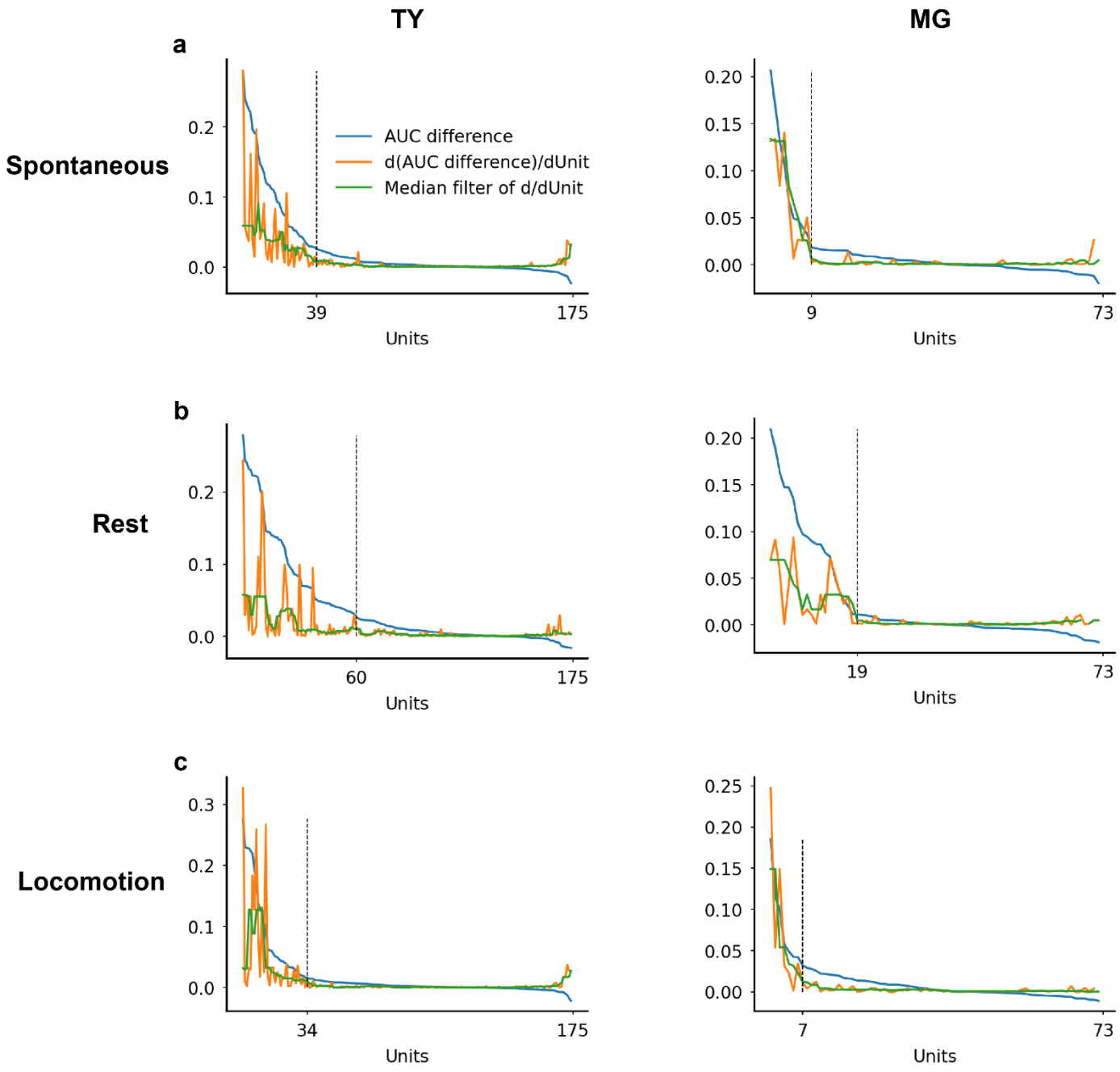

Supplementary Figure 7. Selection of classifier threshold. (A-C) *Left*: TY, *Right:* MG. (A) The difference in AUC between the kinematics + reachFN model and the kinematics + spontaneousFN generalization model was computed for each unit and the differences were sorted by descending value (blue). The derivative of the AUC difference was computed (orange) and smoothed with a median filter (green). Selection of the classifier threshold for separating the context-specific and context-invariant functional groups is based on finding the kink in the plot of AUC difference, which was defined as the unit for which the median-filtered derivative of the AUC difference dropped below 10% of the median of the largest values (12 largest values for TY, 3 largest for MG) in the derivative of AUC difference (in other words, the point at which the marginal change in AUC difference was low for all subsequent units). (B) The difference in AUC and the derivative of the difference between the kinematics + reachFN model and the kinematics + restFN generalization model. (C) The difference in AUC and the derivative of the difference between the kinematics + reachFN model and the kinematics + locomotionFN generalization model.

.

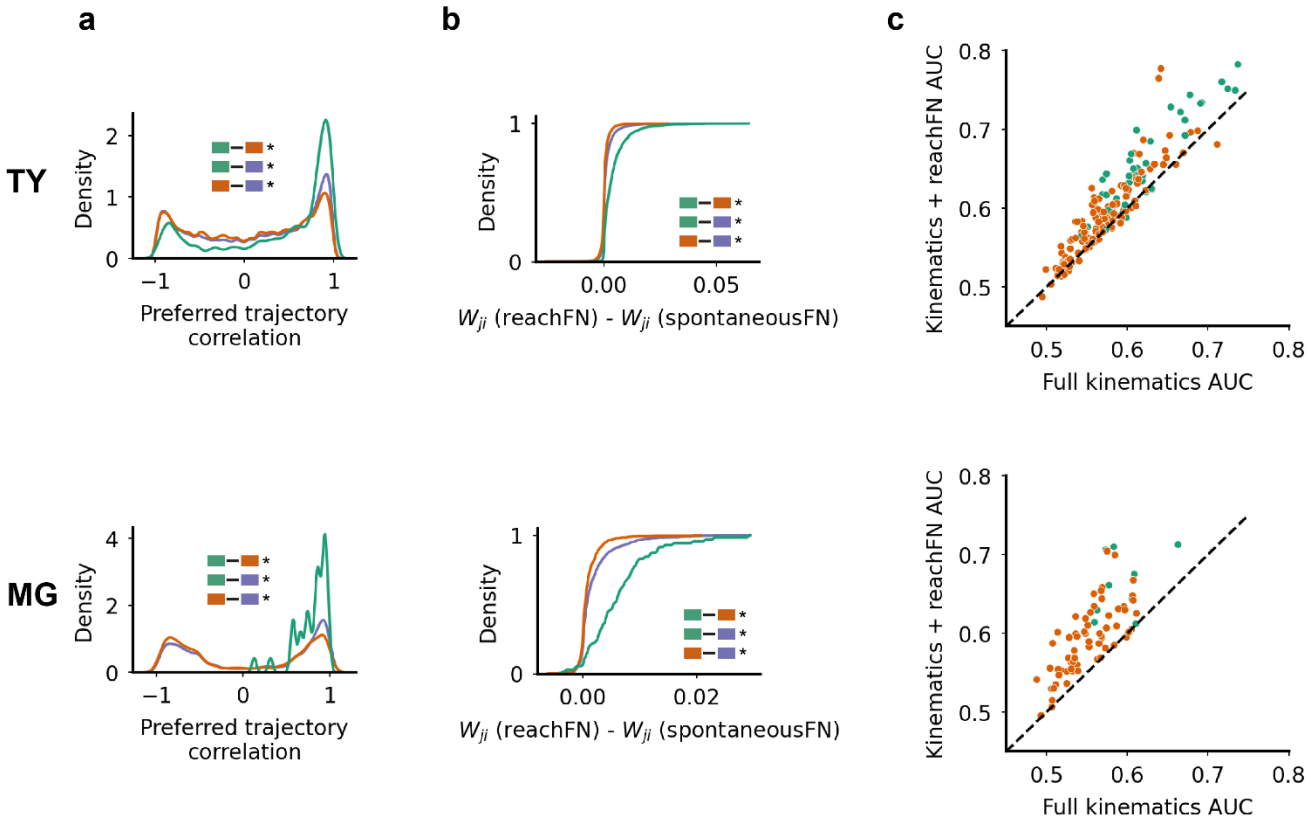

Supplementary Figure 8. Additional context-specific versus context-invariant functional group results. (A) Distributions of preferred trajectory correlations for pairs of units in the full and context-invariant groups that each had full kinematics AUC values greater than the lowest AUC value in the context-specific group, compared to the context-specific group. Legend and statistics are denoted as in Fig. 5 where * indicates significant differences in the median with p<0.01 (two-sided median test) and comparisons without * are not significant (p>0.05). Green, orange, and purple correspond to the context-specific functional group, the context-invariant group, and the full network, respectively. (B) Cumulative distributions of edge weight changes between spontaneousFN and reachFN1 for pairs of units in the same full kinematics AUC-matched set. (C) Scatterplots from Fig. 3a, displayed with hue designating membership in either the context-specific (green) or context-invariant (orange) functional group.

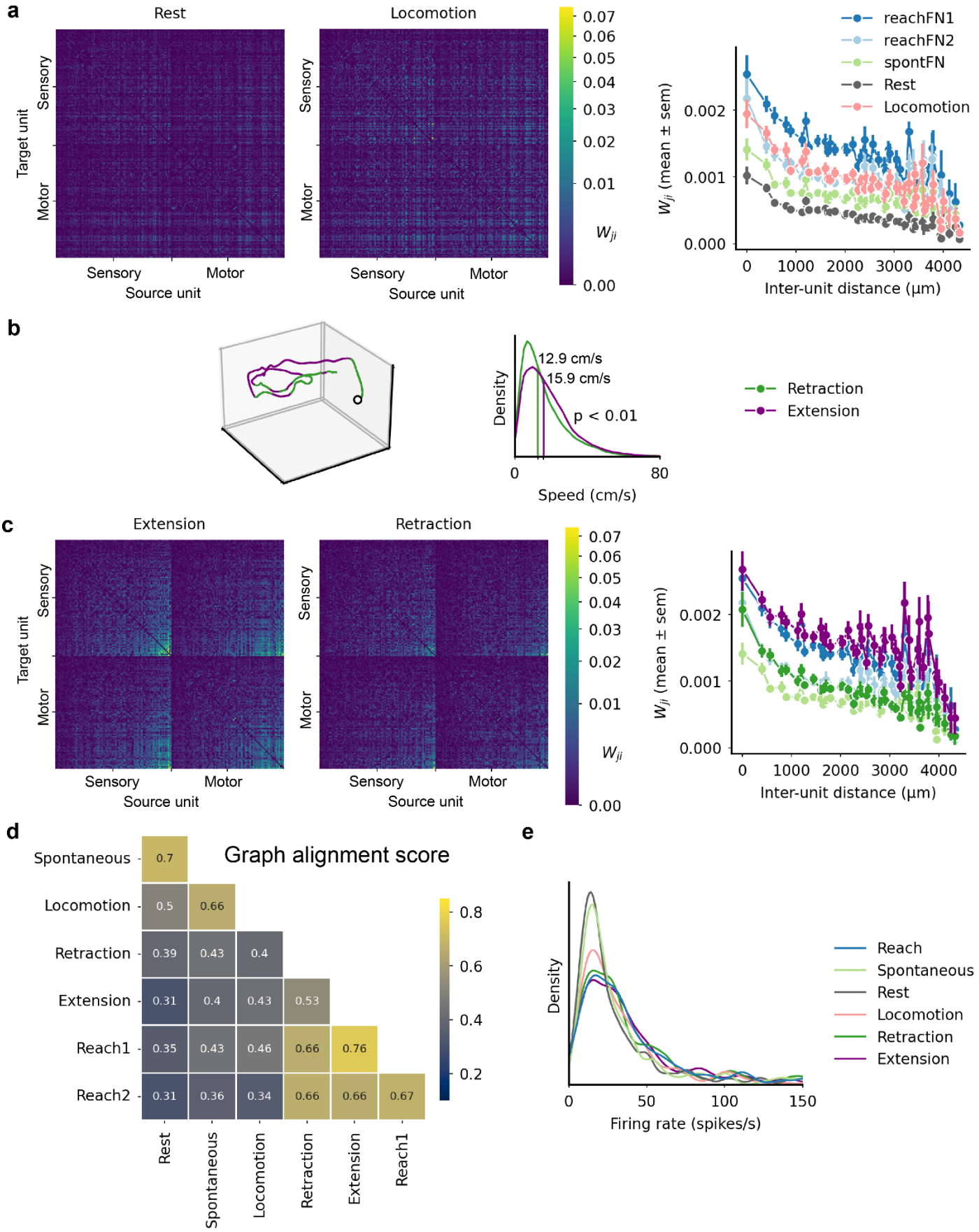

Supplementary Figure 9. Functional networks for rest, locomotion, extension, and retraction in monkey TY. (A) Left: FNs computed from rest and locomotion, with the same unit sorting and color range as in Fig 1d. Right: Reproduction of the bottom right panel of Fig. 1d with weights from the restFN and locomotionFN included for comparison. The sample sizes are equal to those reported in Fig. 1d. (B) Left: extension (purple) and retraction (green) movements marked on the reach shown in Fig. 1b. Right: the distribution of

tangential speeds recorded at all timepoints comprising extension (n=18,300 samples) or retraction (n=19960), with the median speed marked by the vertical line. The median speed during extension is significantly greater than the median speed during retraction according to the median test ($p<0.01$). (C) Left: FNs computed for extension or retraction periods across all reaches. Right: same as the right panel of A, with extension and retraction included for comparison. (D) The graph alignment score between all pairs of FNs. (E) Distributions of firing rates for all units (n=175) during each behavior.

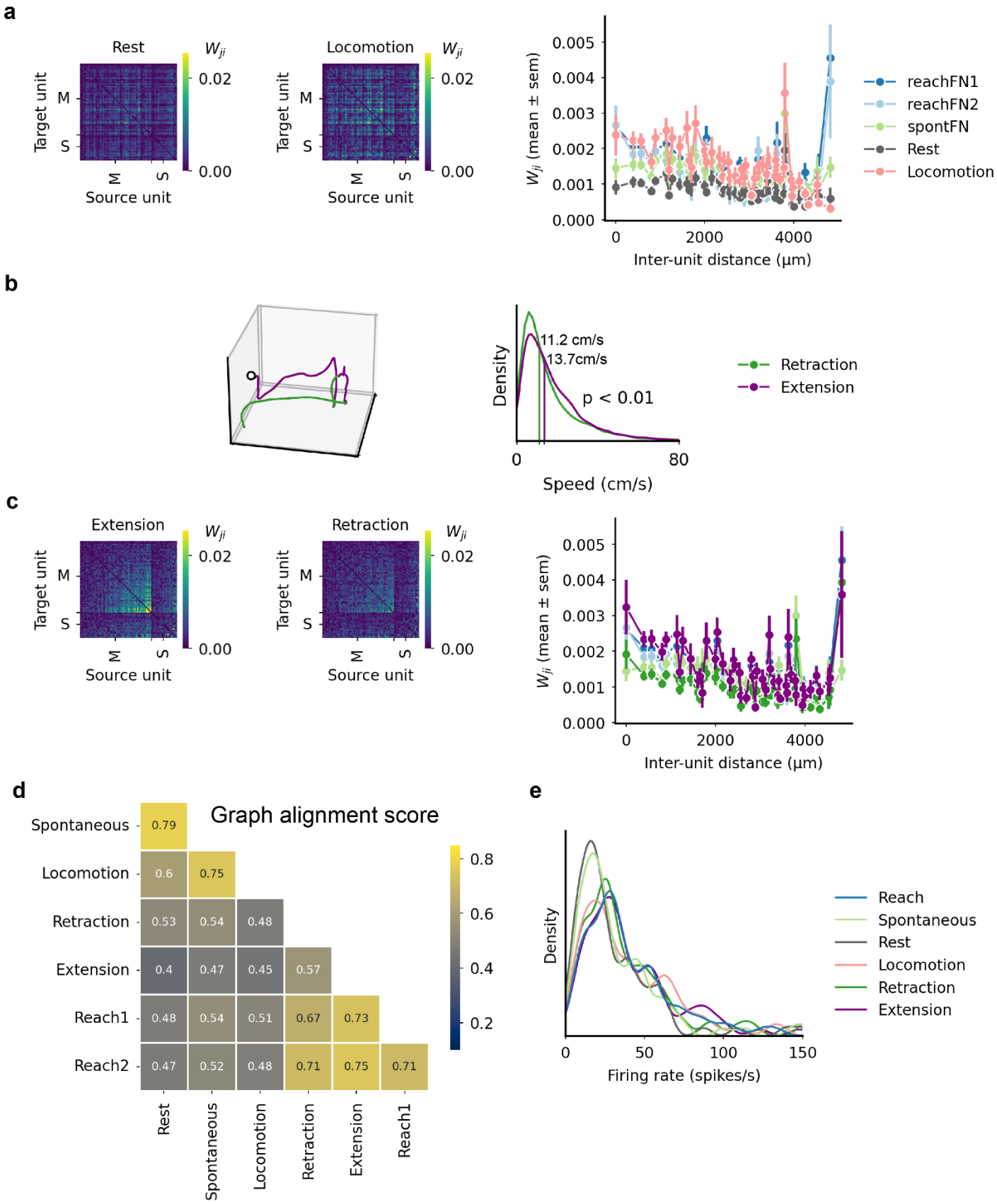

Supplementary Figure 10. Functional networks for rest, locomotion, extension, and retraction in monkey MG. (A-E) Same as Supplementary Fig. 9. In A and C, sample sizes are equal to those reported in Supplementary Fig. 1c. In B, n=13,899 for extension and n=15,672 for retraction. In E, n=73 units for each behavior.

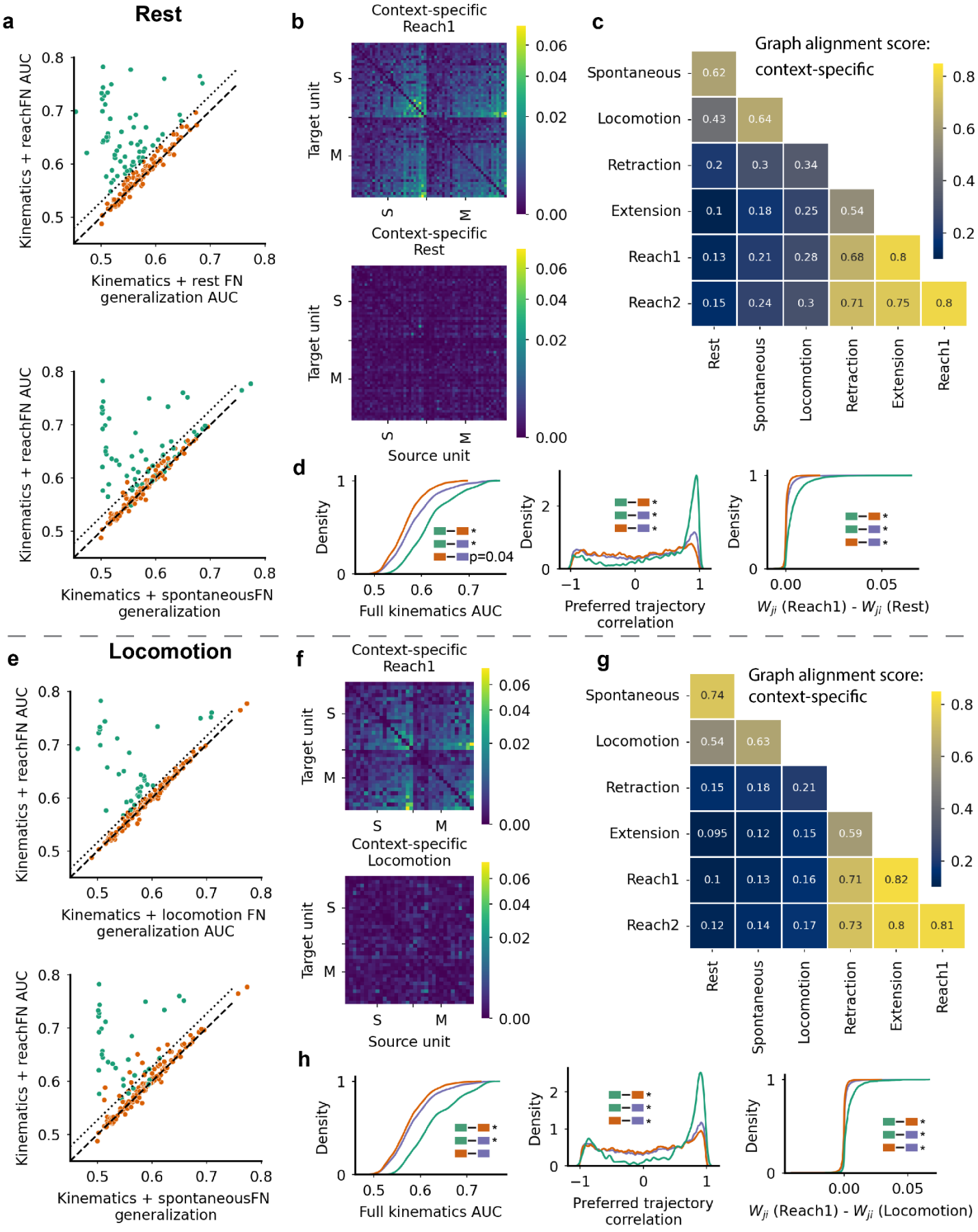

Supplementary Figure 11. Generalization experiments using rest and locomotion FNs, monkey TY. (A) Top: performance of the kinematics + reachFN model versus generalization performance from the kinematics + restFN model. The context-specific group (60/175 units) is in green and the context-invariant group is in orange (115/175 units), with the dotted line denoting the boundary

separating functional groups. Bottom: a reproduction of Fig. 5a, colored by group membership from the restFN generalization experiment shown in the top panel. (B) The context-specific functional group for reachFN1 (top) and rest (bottom). (C) The graph alignment score between pairs of FNs for the context-specific group. (D) Subset of results shown in Figs. 5 and 6 reproduced for the new functional group, with significance of comparisons (all two-sided median tests) shown in the same way. Comparisons of Full Kinematics AUC (left) revealed significant differences between the context-specific and context invariant groups ($p=6.0x10^{-7}$), the context-specific and full groups ($p=5.0x10^{-4}$), and context-invariant and full groups ($p=0.039$). All comparisons of trajectory correlations (middle) revealed significantly different medians with $p\approx0.0$. All comparisons of the difference in weights (right) revealed significantly different medians with $p\approx0.0$. (E-H) Same, for the locomotionFN. The context-specific functional group contains 34 units and the context-invariant group contains 141 units. (H) All comparisons were evaluated with a two-sided median test. Comparisons of Full Kinematics AUC (left) revealed significantly different medians for context-specific and context-invariant groups ($p=0.0010$) and context-specific and full groups ($p=0.0045$), but not for context-invariant and full groups ($p=0.30$). All comparisons of trajectory correlations (middle) revealed significantly different medians with $p\approx0.0$. All comparisons of the difference in weights (right) revealed significantly different medians with $p\approx0.0$.

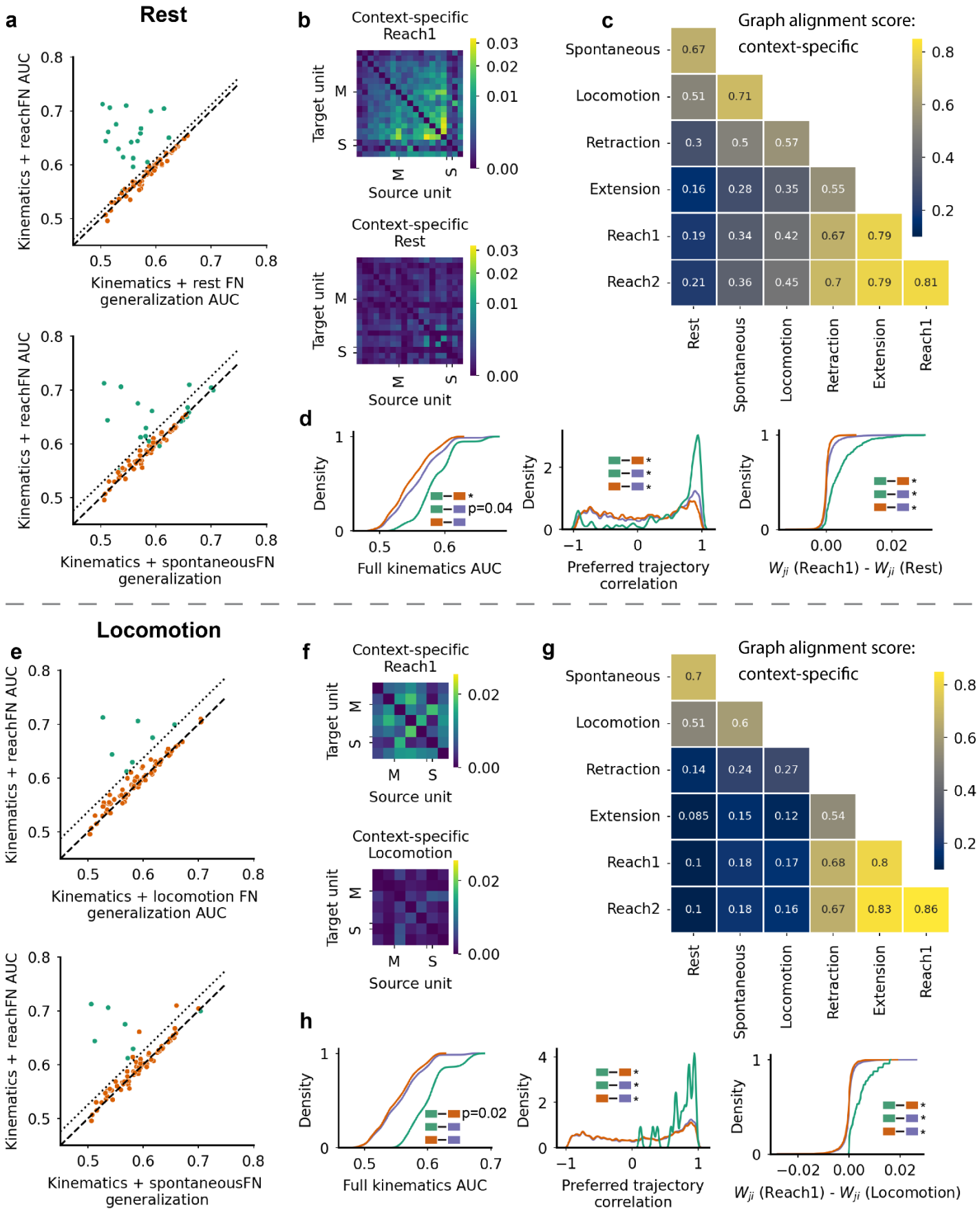

Supplementary Figure 12. Generalization experiments using rest and locomotion FNs, monkey MG. (A-H) Same as Supplementary Fig. 11. The context-specific functional group contains 19 units and the context-invariant group contains 54 units. (D) The comparison of Full Kinematics AUC (left) revealed significant differences between context-specific and. context-invariant functional groups (p=0.0011) and context-specific vs. full (p=0.040), but not for context-invariant vs. full (p=024). All comparisons of trajectory

correlations (middle) revealed significantly different medians with p≈0.0 for all comparisons. All comparisons of the difference in weights (right) revealed significantly different medians with $p=1.4x10^{-43}$, $p=1.0x10^{-34}$, and $p=5.4x10^{-23}$, respectively. (E-H) Same, for the locomotionFN. The context-specific functional group contains 7 units and the context-invariant group contains 66 units. (H) The comparison of Full Kinematics AUC (left) revealed significant differences between context-specific and context-invariant functional groups (p=0.015) but the comparisons of context-specific vs. full (p=0.098) and context-invariant vs. full (p-0.67) revealed no significant difference. All comparisons of trajectory correlations (middle) revealed significantly different medians with p≈0.0 for all comparisons. All comparisons of the difference in weights (right) revealed significantly different medians with $p=5.3x10^{-12}$, $p=4.1x10^{-11}$, and $p=3.3x10^{-8}$, respectively.